

Determinant Monte Carlo for irreducible Feynman diagrams in the strongly correlated regime

Fedor Šimkovic IV.¹ and Evgeny Kozik¹

¹*Department of Physics, King's College London, Strand, London WC2R 2LS, UK*

(Dated: June 10, 2022)

We develop a numerically exact method for efficient summation of irreducible Feynman diagrams for the fermionic self-energy in the thermodynamic limit. The technique, based on the Diagrammatic Determinant Monte Carlo and its recent extension to connected diagrams, allows us to reach unprecedentedly high (~ 10) orders of the weak-coupling expansion for the self-energy of the two-dimensional Hubbard model. Access to high orders reveals a non-trivial analytic structure of the self-energy and enables its controlled reconstruction with arbitrary momentum resolution in the non-perturbative regime of essentially strong correlations, which has recently been reached with ultracold atoms in optical lattices.

Definitive answers to key questions about various forms of collective behavior of interacting electrons—from quantum magnetism to photovoltaics and high-temperature superconductivity—hinge upon our ability to describe their properties reliably, i.e. without having to introduce uncontrolled systematic errors. This understanding has led to a surge of interest in development of unbiased computational approaches for correlated fermions and the problem of controlling their error bars, which has become the focus of concerted effort (see, e.g., Ref. [1] and references therein). Such systematic studies reinforce the view that there is no single universal technique that could access all aspects of correlation physics in different regimes at once.

Quantum Monte Carlo techniques on a lattice [2–5] are very powerful at fermion densities around one particle per site (half filling), and moderate coupling, but struggle to control the error bars in the thermodynamic limit at low temperatures and non-zero doping. Controllable approaches based on systematic extensions of the dynamical mean-field theory [6–8] are particularly effective whenever the observable is not sensitive to long-range correlations. Diagrammatic Monte Carlo (DiagMC) techniques [9–13] stochastically sum all Feynman diagrams to a high order immediately in the thermodynamic limit and can reliably capture non-trivial spatial correlations, but their controllability depends on convergence properties of the series, which typically diverges already at moderate interaction strengths. The current state of the field is that perhaps the most interesting regime of moderate-to-strong interactions, which is expected to harbour non-trivial correlation physics at relatively high temperatures, is hardly under control by any available computational method.

With the lack of accurate theoretical solutions, a promising approach is experimental emulation of basic models of correlated electrons in solids, in particular with ultracold atoms loaded in an optical lattice [14–23]. This field has seen dramatic progress since the realisation [16, 18, 19] of the prototypical fermionic Hubbard

model [24–27]

$$H = -t \sum_{\langle i,j \rangle \sigma} \hat{c}_{i,\sigma}^\dagger \hat{c}_{j,\sigma} + U \sum_i \hat{n}_{i,\uparrow} \hat{n}_{i,\downarrow} - \sum_{i,\sigma} \mu_\sigma \hat{n}_{i,\sigma}, \quad (1)$$

where μ_σ is the chemical potential, $\hat{c}_{i,\sigma}^\dagger$ and $\hat{c}_{i,\sigma}$ create and annihilate (respectively) a fermion with the spin $\sigma \in \{\uparrow, \downarrow\}$ on the site i , and $\hat{n}_{i,\sigma} = \hat{c}_{i,\sigma}^\dagger \hat{c}_{i,\sigma}$. Until recently, this model has been studied at relatively high temperatures, where several theoretical approaches provide reliable benchmarks for calibration and cross-validation of results. However, substantial progress of cooling and probing techniques has already allowed access to sufficiently low temperatures to observe magnetic properties [20–22], and, very recently, detect long-range antiferromagnetic correlations in the 2D Hubbard model at temperatures as low as $T = 0.25t$ and $U \approx 7t$. The experiments have thus already reached the most challenging regime for all current theoretical methods.

Here, we introduce a numerically exact approach for stochastic summation of irreducible Feynman diagrams for the fermionic self-energy based on Diagrammatic Determinant Monte Carlo (DDMC) [3–5] and its recent extension to connected diagrams in the thermodynamic limit (CDet) [13], Σ DDMC. The method allows us to reach unprecedentedly high orders of the diagrammatic series for the self-energy of the two-dimensional Hubbard model (1) immediately in the thermodynamic limit. Although the series manifestly diverges in strongly correlated regimes, access to high orders enables a systematic protocol for reconstructing the self-energy with controlled accuracy and arbitrary momentum resolution. We demonstrate the technique for typical parameters $U = 7t$, $T = 0.2t$, $\mu = 2t$ (density $n = 0.950(6)$, we set $t = 1$ below), the regime where other methods are currently struggling to reach a controlled solution [1], and use it to obtain the corresponding (quasi-)momentum distribution, which can be observed experimentally.

We start from the effective action with the arbitrary free parameter α [3, 4, 28, 29] and the expansion variable

ξ ,

$$S_\xi = - \sum_{\omega_n, \mathbf{k}, \sigma} c_{\omega_n, \mathbf{k}, \sigma}^\dagger G_\sigma^{(0)}(i\omega_n, \mathbf{k})^{-1} c_{\omega_n, \mathbf{k}, \sigma} \quad (2)$$

$$- \xi \sum_{\omega_n, \mathbf{k}, \sigma} \alpha_\sigma c_{\omega_n, \mathbf{k}, \sigma}^\dagger c_{\omega_n, \mathbf{k}, \sigma} + \xi U \int_0^\beta n_{\tau\uparrow} n_{\tau\downarrow} d\tau,$$

where $G_\sigma^{(0)}(i\omega_n, \mathbf{k})^{-1} = i\omega_n + \mu_\sigma - \epsilon_{\mathbf{k}\sigma} - \alpha_\sigma$ and $\epsilon_{\mathbf{k}\sigma}$ is the dispersion relation of the non-interacting system. At $\xi = 1$ the action corresponds to the Hamiltonian (1). Expansion in powers of ξ and application of Wick's theorem leads to the diagrammatic series for the partition function Z (see, e.g., Ref. [30]). The key observation [3, 4] is that the sum of all $(n!)^2$ diagrams of order n for a given configuration $\mathcal{S}_n = \{\mathbf{x}_j, j = 1, \dots, n\}$ of n vertices in space-imaginary time, $\mathbf{x}_j = (\mathbf{x}_j, \tau_j)$, can be recovered from the product of two determinants

$$z(\mathcal{S}_n) = \det A^\uparrow(\mathcal{S}_n) \det A^\downarrow(\mathcal{S}_n), \quad (3)$$

where the matrices A^σ are constructed from the Green's functions, $A_{ij}^\sigma(\mathcal{S}_n) = G_\sigma^{(0)}(\mathbf{x}_j - \mathbf{x}_i) - (\alpha_\sigma/U)\delta_{ij}$. Thus, the net contribution of the factorial number of diagrams of order n can be computed in only $\mathcal{O}(n^3)$ elementary operations, and the sum over all possible \mathcal{S}_n can be efficiently sampled by Monte Carlo [3–5]. Nonetheless, although the series for Z converges for any finite volume V and inverse temperature $\beta = 1/T$, the average diagram order grows as $\beta V U$, and in typical interesting cases the extrapolation to the thermodynamic limit is practically impossible. This is because the sum (3) is dominated by disconnected diagrams—those containing pieces that are not linked to the rest of the diagram by a $G^{(0)}$ line—responsible for the exponential scaling of Z on βV .

A family of DiagMC techniques, stochastically summing only the connected (and typically also irreducible [31]) diagrams [9, 10, 12], enables calculation of dynamical observables, such as the fermionic self-energy $\Sigma_{\mathbf{k}\sigma}$, $\mathbf{k} = (\mathbf{k}, -i\omega_n)$, immediately in the thermodynamic limit. However, until recently, these diagrams have been sampled in DiagMC one by one, constituting a factorial scaling of computational time with the diagram order n . While diagram orders as high as $n \sim 6$ could be accessed in practice, it is typically insufficient for obtaining controlled results at strong correlations. It is therefore tempting to take advantage of the determinantal summation in the spirit of Eq. (3) for series of irreducible diagrams as well.

It was shown recently that determinantal summation could be applied to series of *connected* diagrams immediately in the thermodynamic limit [13]. The idea is that for each configuration of vertices \mathcal{S}_n in Eq. (3) one can recursively subtract all the disconnected diagrams, constructed from determinants of principal submatrices of A^σ . While all possible diagrams of order n take $\mathcal{O}(n^3)$ elementary operations to sum by a single determinant, extracting only the connected ones requires computing determinants for all proper subsets of

\mathcal{S}_n , which is $\mathcal{O}(n^3 2^n)$ steps, and a number of subtractions that grows exponentially as $\mathcal{O}(3^n)$ [13]. Nonetheless, it beats the factorial scaling of DiagMC in the theoretical large- n limit. Most importantly, it was shown that in practice this trick allows to reach diagram orders as high as $n \sim 10$ for the grand potential density and obtain the pressure with unmatched accuracy in the weakly correlated regime ($U \sim 2$). The approach of determinantal summation/subtraction can be extended to sums of irreducible diagrams for the self-energy, as we shall see, at an exponential cost as well. The question remains, however, of whether it can bring any practical benefits in terms of enabling access to the regime of truly strong correlations.

The series for the self-energy $\Sigma_{\mathbf{k}\sigma}$ consists of all possible connected irreducible diagrams with two vertices that lack their respective incoming/outgoing propagators with spin σ and four-(quasi)-momentum \mathbf{k} [30]. For a particular vertex configuration \mathcal{S}_n , we can compute the sum of all $(n!)^2$ diagrams (including disconnected and reducible) with two open ends carrying σ and \mathbf{k} by

$$z_{\mathbf{k}\sigma}(\mathcal{S}_n, l: x_l) = \det A_{\mathbf{k}}^\sigma(\mathcal{S}_n, l: x_l) \det A^{\bar{\sigma}}(\mathcal{S}_n), \quad (4)$$

where the matrix $A_{\mathbf{k}}^\sigma(\mathcal{S}_n, j: \mathbf{x})$ is obtained from $A^\sigma(\mathcal{S}_n)$ by replacing its j -th column by the vector $(e^{i\mathbf{k}\cdot(\mathbf{x}-\mathbf{x}_1)}, e^{i\mathbf{k}\cdot(\mathbf{x}-\mathbf{x}_2)}, \dots, e^{i\mathbf{k}\cdot(\mathbf{x}-\mathbf{x}_n)})^\top$, and $\sigma \neq \bar{\sigma}$. Now the task is to remove from $z_{\mathbf{k}\sigma}$ all the disconnected and reducible diagrams. To this end, we define an auxiliary quantity

$$f_\sigma(\mathcal{S}_n, l: \mathbf{x}) = \det A_G^\sigma(\mathcal{S}_n, l: \mathbf{x}) \det A^{\bar{\sigma}}(\mathcal{S}_n), \quad (5)$$

with the matrix $A_G^\sigma(\mathcal{S}_n, l: \mathbf{x})$ obtained from $A^\sigma(\mathcal{S}_n)$ by replacing x_l in its l -th column by \mathbf{x} . In essence, f_σ sums all the diagrams of the general structure $z \Sigma(\mathbf{x}_{i_1} - x_l) G^{(0)}(\mathbf{x}_{i_2} - \mathbf{x}_{i_1}) \dots \Sigma(\mathbf{x}_{i_p} - \mathbf{x}_{i_{p-1}}) G^{(0)}(\mathbf{x} - \mathbf{x}_{i_p})$, which start at the self-energy vertex x_l from the set \mathcal{S}_n , end with a propagator going to the external vertex \mathbf{x} , and may have disconnected parts z . Thus, the sum of all self-energy diagrams for the configuration \mathcal{S}_n can be obtained recursively from the formula:

$$s_{\mathbf{k}\sigma}(\mathcal{S}_n, l: x_l) = z_{\mathbf{k}\sigma}(\mathcal{S}_n, l: x_l) - \sum_{\mathcal{S}_p \subset \mathcal{S}_n: x_l \in \mathcal{S}_p} z(\mathcal{S}_n \setminus \mathcal{S}_p) s_{\mathbf{k}\sigma}(\mathcal{S}_p, l: x_l)$$

$$- \sum_{\mathcal{S}_p \subset \mathcal{S}_n: x_l \in \mathcal{S}_p} \sum_{x_m \in (\mathcal{S}_n \setminus \mathcal{S}_p)} f_\sigma(\mathcal{S}_p, l: x_m) s_{\mathbf{k}\sigma}(\mathcal{S}_n \setminus \mathcal{S}_p, m: x_l) \quad (6)$$

Here $x_l \in \mathcal{S}_n$, the first sum is over proper subsets \mathcal{S}_p of \mathcal{S}_n that include x_l , the last term is additionally summed over all vertices x_m that belong to \mathcal{S}_n but not to \mathcal{S}_p .

Finally, the expansion of $\Sigma_{\mathbf{k}\sigma}$ in powers of ξ (we restore the explicit dependence on external parameters) reads

$$\Sigma_{\mathbf{k}\sigma}(T, \mu, U) = \sum_{n=1}^{\infty} a_{n, \mathbf{k}\sigma}(T, \mu_\sigma - \alpha_\sigma, \alpha_\sigma/U) (U\xi)^n, \quad (7)$$

with the coefficients

$$a_{n, \mathbf{k}\sigma} = \frac{(-1)^n}{n!} \sum_{\mathcal{S}_n, l} s_{\mathbf{k}\sigma}(\mathcal{S}_n, l: x_l), \quad (8)$$

where $\sum_{\mathcal{S}_n} = \sum_{\mathbf{x}_1 \dots \mathbf{x}_n} \prod_{j=1}^n \int_0^{1/T} d\tau_j$. The sum over all vertex configurations can be efficiently computed by the standard continuous-time Metropolis-type scheme (see, e.g. Ref. [32] for details). At each Monte Carlo step, the evaluation of $s_{\mathbf{k}\sigma}$ is done in two stages: first, all determinants involved in Eq. (6) are computed in $\mathcal{O}(n^5 2^n)$ elementary operations, then the recursive procedure (6) is performed in $\mathcal{O}(n^2 3^n)$ steps. This scaling could be improved: the tree algorithm [33, 34] and fast subset convolution [35] reduce these costs to $\mathcal{O}(n^2 2^n)$ and $\mathcal{O}(n^4 2^n)$ [$\mathcal{O}(2^n)$ and $\mathcal{O}(n^2 2^n)$ for CDet [34]] respectively. For realistically accessible orders ($n \sim 12$) the computational cost of both approaches is comparable. Given \mathcal{S}_n , our code evaluates the sum of all 24936416 irreducible diagrams at $n = 10$ [34] averaged over 10! permutations of vertices in ~ 0.01 s on modern CPU.

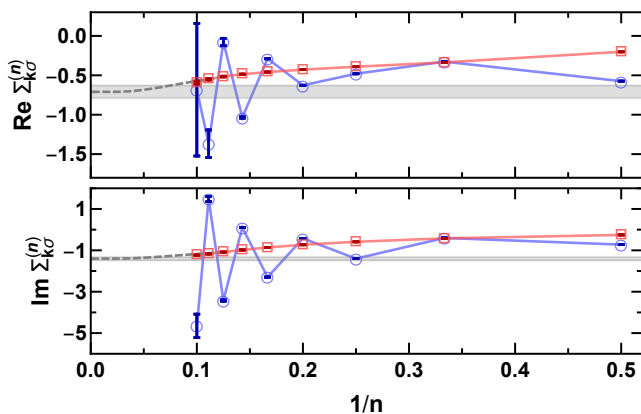


Figure 1. (color online) Partial sum $\Sigma_{\mathbf{k}\sigma}^{(n)}$ of the original expansion (7) at $\xi = 1$ (circles) and that in terms of the transformed variable $w(\xi)$ (squares) at $T = 0.2t$, $U = 7t$, $\mu = 2t$, $\omega = \omega_0$, $\mathbf{k} = [\pi, 0.4]$ as a function of inverse truncation order. The horizontal bands are the claimed result, Fig. 3.

We now turn to the problem of reconstructing $\Sigma_{\mathbf{k}\sigma}$ given the series coefficients a_n obtained by Σ DDMC. Note that, by construction, $\Sigma_{\mathbf{k}\sigma}$ does not depend on the choice of α , but the series is different for each α , which can be used, e.g., to control its convergence [28, 29]. Here we use this freedom to maximise the order n we can reach, which empirically amounts to nullifying the diagonal of A^σ , so that α is found from $G_\sigma^{(0)}(\mathbf{x} = 0, \tau = -0) = \alpha/U$. For method validation, we have reproduced current state-of-the-art benchmarks [1, 29]. Here, we address an essentially correlated regime, where controlled results for $\Sigma_{\mathbf{k}\sigma}$ in the thermodynamic limit are not accessible by other methods [1]. The result of the partial sum $\Sigma^{(n)} = \sum_{m=0}^n a_m U^m$ at the lowest Matsubara frequency ω_0 and $\mathbf{k} = [\pi, 0.4]$ as a function of n up to $n_{\max} = 10$, shown in Fig. 1, evidences that the series is wildly divergent. It is known, however, [9, 10, 36] that the series (7) at $T > 0$ generally has a non-zero convergence radius. Except special cases, the position of the

singularity closest to the origin in the complex plane of the expansion parameter ξ can be found from the ratio test, $U_{\xi s_1} = \lim_{n \rightarrow \infty} a_{n-1}/a_n$. Fig. 2 shows a_{n-1}/a_n as a function of n , suggesting $U_{\xi s_1} \approx -5$.

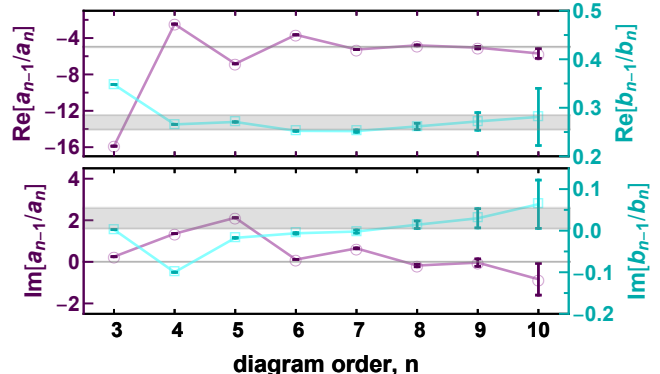


Figure 2. (color online) The ratio of successive coefficients of the original, a_{n-1}/a_n (circles), and transformed by the map $w(\xi)$, b_{n-1}/b_n (squares), series for the parameters of Fig. 1. The first singularity is observed at $U_{\xi s_1} \approx -5$ and the second one at $w_{s_2} \approx 0.27 + i0.03$ (corresponding to $U_{\xi s_2} \approx -9$), while $w(\xi = 1) = 0.23$.

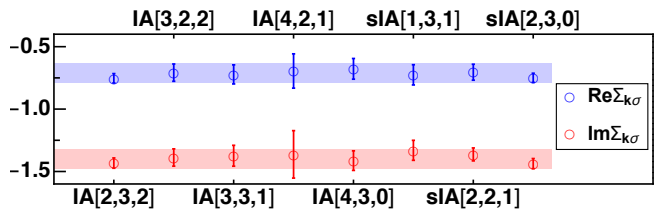


Figure 3. (color online) Evaluation of $\Sigma_{\mathbf{k}\sigma}$ for the parameters of Fig. 1 using the IA method (9) applied to the series (7) (labelled IA) and the shifted series for Σ/ξ^2 (sIA) for various choices of $[L, M, N]$. The horizontal bands show the claimed result with the error bar.

The singularity with $\text{Re}\xi_{s_1} < 0$ is an inconvenience, but does not prevent one from accurately obtaining the self-energy at $\xi = 1$. A standard approach is analytic continuation based on conformal maps. Given $\Sigma(\xi)$, which is analytic at $\xi = 0$ in the open disk $|\xi| < |\xi_{s_1}|$, the idea is to transform the complex plane of ξ using an analytic function $w = w(\xi)$, $w(0) = 0$, to a domain of the complex variable w where the singularity is farther away from the origin than the image of $\xi = 1$, $|w(\xi_{s_1})| > |w(1)|$. As a function of w , $\Sigma(\xi(w))$ is then analytic at $w = 0$ in the open disk $|w| < |w(\xi_{s_1})|$, which now contains $w(1)$. Re-expanding $\sum_n a_n (\xi(w))^n$ in powers of w , we obtain $\Sigma(\xi) = \sum_n b_n (w(\xi))^n$, which converges at $\xi = 1$.

Such a map is not unique. We choose $\xi = -4\xi_{s_1} w / (1 - w)^2$, which maps the disk $|w| < 1$ onto the complex plane of ξ with a branch cut along the real axis from ξ_{s_1} to

$-\infty$. The coefficients b_n determine the position of the next singularity nearest to the origin w_{s_2} . The plateau of b_{n-1}/b_n at $n \gtrsim 7$, Fig. 2, gives w_{s_2} and confirms that the expansion in w is indeed convergent, $|w_{s_2}| > |w(1)|$. This observation is key for a controlled extrapolation of Σ w.r.t. $n \rightarrow \infty$, which would be impossible with current DiagMC, typically cut off at $n \sim 6$. Depending on the map, singularities other than ξ_{s_2} can appear closer to the origin and will manifest themselves in b_{n-1}/b_n . The configuration of singularities generally changes with \mathbf{k} .

To evaluate the series, we use the Integral Approximant [37] (IA) technique [38], which associates the result with the function $g(w)$, $\Sigma = g(w(1))$, that has the same Taylor series as $\Sigma(w)$ up to the highest accessible order n_{\max} and satisfies the differential equation

$$Q_M(x)g'(x) + P_L(x)g(x) + R_N(x) = 0. \quad (9)$$

Here Q, P, R are polynomials of orders M, L, N , respectively, determined as the unique solution of Eq. (9) for $g(x) = \sum_{n=0}^{n_{\max}} b_n x^n$ up to terms $\mathcal{O}(x^{M+N+L+2})$ with $M + N + L + 2 = n_{\max}$. In effect, Eq. (9) continues the (not necessarily convergent) series for $g(x)$ from $n \leq n_{\max}$ to infinite order and reconstructs the function behind it. The IA approach reduces to other standard resummation methods, such as, e.g., Padé [39] and Dlog-Padé [40], as special cases [38], capturing a more general analytic structure with algebraic singularities: near the singular point x_s (a zero of $Q_M(x)$) $g(x) = \phi_1(x)(1-x/x_s)^{-\nu} + \phi_2(x)$, with functions $\phi_{1,2}(x)$ regular at x_s .

The resummation (9) can also be used to obtain Σ or Σ/ξ^2 (since $a_0 = a_1 = 0$) directly from the divergent series (7), Fig. 3. In this case, Q, P, R are constructed for $g(x) = \sum_{n=0}^{n_{\max}} a_n x^n$ or $g(x) = \sum_{n=2}^{n_{\max}} a_n x^{n-2}$ respectively. We verify that the bias introduced by the extrapolation (9) is negligible by observing that the discrepancy between the estimates of Σ obtained for different appropriate [38] choices of $[L, M, N]$ is negligible compared to the corresponding statistical error. Vice versa, a measurable deviation from the assumed asymptotic form (9) would manifest itself as an inconsistency between different IAs beyond error bars. The results are in perfect agreement with those obtained for the transformed series (not shown), providing further evidence that the systematic error of the adopted resummation procedure is negligible. As a by-product, the procedure yields an estimate of the nearest singularity location, $U\xi_{s_1} = (-5.7(3) - i0.2(8))$, which may correspond to the s-wave superfluid transition [13] (at a different density in view of Eq. 7). Since our $\{a_n\}$ ($\{b_n\}$) have error bars, we found that approximants with more general asymptotics, such as, e.g., hypergeometric/Meijer- G [41, 42] or Borel-Padé/Borel-Dlog-Padé [43, 44], result in large uncertainty of the extrapolation unless additional constraints on the number or form of singularities are introduced [45].

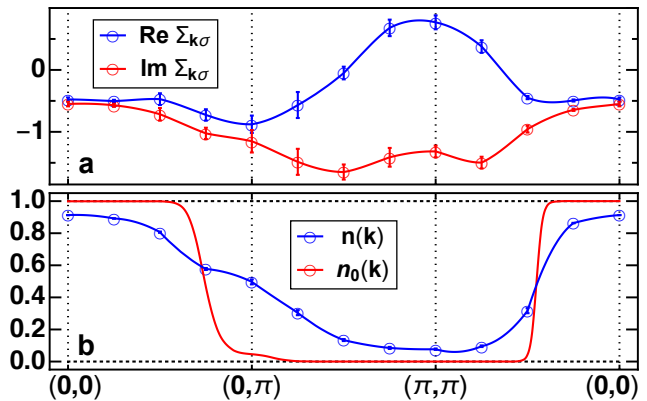


Figure 4. (color online) (a) $\Sigma_{\mathbf{k}\sigma}$ at $\omega = \omega_0$; (b) the corresponding momentum distribution $n(\mathbf{k})$ at $T = 0.2t$, $U = 7t$, $\mu = 2t$ ($n = 0.950(6)$) and $n_0(\mathbf{k})$ of the ideal Fermi gas, $U = 0$.

We follow this protocol to map out the momentum dependence of $\Sigma_{\mathbf{k}\sigma}$ at $\omega = \omega_0$, Fig. 4a. The knowledge of the self-energy allows to obtain an accurate estimate of the momentum distribution $n(\mathbf{k}) = \langle c_{\mathbf{k}}^\dagger c_{\mathbf{k}} \rangle$ via the Dyson equation [30], Fig. 4b. We found that this approach leads to a more accurate estimate for $n(\mathbf{k})$ than computing it directly with CDet. The shape of $n(\mathbf{k})$ is qualitatively different from that of the corresponding non-interacting Fermi gas ($U = 0$), revealing that the system is of strongly-correlated non-Fermi liquid character. The function $n(\mathbf{k})$ can be straightforwardly probed experimentally with ultracold atoms in optical lattices [15], which have recently been brought to this regime of parameters [23]. Our data thus provide a controlled theoretical benchmark for the ongoing studies of strong correlations in the 2D Hubbard model.

In conclusion, we note that, following Ref. [46], the exponential computational cost of Σ DDCM with the observation that the transformed series converges solves the fermion negative sign problem [47]: the computational time scales polynomially with the inverse of the desired error bar. In addition to controlled determination of observables in regimes analytically connected to the non-interacting limit, the diagrammatic approach offers a unique means of detecting and analysing phase transitions. Being fundamentally free from finite-size effects, the series (7) is bound to diverge at a point of non-analyticity. The key result is that $n \sim 10$ accessed by Σ DDMC appears to be in the asymptotic regime at least at $T \sim 0.2$, meaning that the point of non-analyticity and potentially certain critical properties can be found from the analysis of a_n suggested above.

While this paper was under review, a similar to Eqs. (4)-(8) algorithm was published [48], applied in a regime where the series converges. An alternative approach was subsequently proposed in Ref. [49].

We are grateful to Michel Ferrero and Alice Moutenet for discussions of the algorithm and to Aaram J. Kim, Héctor Mera and Branislav Nikolić for discussions of resummation techniques. This work was supported by the Simons Collaboration on the Many Electron Problem and by EPSRC through the grant EP/P003052/1.

-
- [1] J. P. F. LeBlanc, A. E. Antipov, F. Becca, I. W. Bulik, G. K.-L. Chan, C.-M. Chung, Y. Deng, M. Ferrero, T. M. Henderson, C. A. Jiménez-Hoyos, E. Kozik, X.-W. Liu, A. J. Millis, N. V. Prokof'ev, M. Qin, G. E. Scuseria, H. Shi, B. V. Svistunov, L. F. Tocchio, I. S. Tupitsyn, S. R. White, S. Zhang, B.-X. Zheng, Z. Zhu, and E. Gull (Simons Collaboration on the Many-Electron Problem), *Phys. Rev. X* **5**, 041041 (2015).
- [2] R. Blankenbecler, D. J. Scalapino, and R. L. Sugar, *Phys. Rev. D* **24**, 2278 (1981).
- [3] A. Rubtsov, arXiv:cond-mat/0302228. (2003).
- [4] A. N. Rubtsov, V. V. Savkin, and A. I. Lichtenstein, *Phys. Rev. B* **72**, 035122 (2005).
- [5] E. Burovski, N. Prokof'ev, B. Svistunov, and M. Troyer, *New Journal of Physics* **8**, 153 (2006).
- [6] A. Georges, G. Kotliar, W. Krauth, and M. J. Rozenberg, *Rev. Mod. Phys.* **68**, 13 (1996).
- [7] G. Kotliar, S. Y. Savrasov, G. Pálsson, and G. Biroli, *Phys. Rev. Lett.* **87**, 186401 (2001).
- [8] T. Maier, M. Jarrell, T. Pruschke, and M. H. Hettler, *Rev. Mod. Phys.* **77**, 1027 (2005).
- [9] K. Van Houcke, E. Kozik, N. Prokofev, and B. Svistunov, *Physics Procedia* **6**, 95 (2010).
- [10] E. Kozik, K. Van Houcke, E. Gull, L. Pollet, N. Prokof'ev, B. Svistunov, and M. Troyer, *EPL (Europhysics Letters)* **90**, 10004 (2010).
- [11] K. Van Houcke, F. Werner, E. Kozik, N. Prokof'ev, B. Svistunov, M. J. H. Ku, A. T. Sommer, L. W. Cheuk, A. Schirotzek, and M. W. Zwierlein, *Nature Physics* **8**, 366 EP (2012).
- [12] Y. Deng, E. Kozik, N. V. Prokof'ev, and B. V. Svistunov, *EPL (Europhysics Letters)* **110**, 57001 (2015).
- [13] R. Rossi, *Phys. Rev. Lett.* **119**, 045701 (2017).
- [14] D. Jaksch, C. Bruder, J. I. Cirac, C. W. Gardiner, and P. Zoller, *Physical Review Letters* **81**, 3108 (1998).
- [15] I. Bloch, *Nature Physics* **1**, 23 EP (2005).
- [16] M. Köhl, H. Moritz, T. Stöferle, K. Günter, and T. Esslinger, *Physical Review Letters* **94**, 080403 (2005).
- [17] M. Lewenstein, A. Sanpera, V. Ahufinger, B. Damski, A. Sen, and U. Sen, *Advances in Physics* **56**, 243 (2007).
- [18] R. Jördens, N. Strohmaier, K. Günter, H. Moritz, and T. Esslinger, *Nature* **455**, 204 (2008).
- [19] U. Schneider, L. Hackermüller, S. Will, T. Best, I. Bloch, T. Costi, R. Helmes, D. Rasch, and A. Rosch, *Science* **322**, 1520 (2008).
- [20] R. G. Hulet, P. M. Duarte, R. A. Hart, and T.-L. Yang, in *Laser Spectroscopy* (2016) pp. 43–49.
- [21] D. Greif, G. Jotzu, M. Messer, R. Desbuquois, and T. Esslinger, *Physical Review Letters* **115**, 260401 (2015).
- [22] M. F. Parsons, A. Mazurenko, C. S. Chiu, G. Ji, D. Greif, and M. Greiner, *Science* **353**, 1253 (2016).
- [23] A. Mazurenko, C. S. Chiu, G. Ji, M. F. Parsons, M. Kanász-Nagy, R. Schmidt, F. Grusdt, E. Demler, D. Greif, and M. Greiner, *Nature* **545**, 462 EP (2017).
- [24] J. Hubbard, in *Proceedings of the royal society of london a: mathematical, physical and engineering sciences*, Vol. 276 (The Royal Society, 1963) pp. 238–257.
- [25] P. W. Anderson, *Solid state physics* **14**, 99 (1963).
- [26] P. W. Anderson *et al.*, *The theory of superconductivity in the high-Tc cuprate superconductors*, Vol. 446 (Princeton University Press Princeton, NJ, 1997).
- [27] P. A. Lee, N. Nagaosa, and X.-G. Wen, *Rev. Mod. Phys.* **78**, 17 (2006).
- [28] R. E. V. Profumo, C. Groth, L. Messio, O. Parcollet, and X. Waintal, *Phys. Rev. B* **91**, 245154 (2015).
- [29] W. Wu, M. Ferrero, A. Georges, and E. Kozik, *Phys. Rev. B* **96**, 041105 (2017).
- [30] A. A. Abrikosov, L. P. Gor'kov, and I. E. Dzyaloshinski, *Methods of Quantum Field Theory in Statistical Physics* (Dover Publications Inc., 1975).
- [31] Here, by irreducible we mean those diagrams that can not be split into two disconnected pieces by cutting any fermionic line.
- [32] E. Kozik, E. Burovski, V. W. Scarola, and M. Troyer, *Phys. Rev. B* **87**, 205102 (2013).
- [33] K. Griffin and M. J. Tsatsomeris, *Linear Algebra and its Applications* **419**, 107 (2006).
- [34] F. Šimkovic IV, PhD Thesis (2018).
- [35] A. Bjrklund, T. Husfeldt, P. Kaski, and M. Koivisto (2007) pp. 67–74.
- [36] G. Benfatto, A. Giuliani, and V. Mastropietro, *Annales Henri Poincaré* **7**, 809 (2006).
- [37] Sometimes called Differential Approximant.
- [38] D. Hunter and G. A. Baker Jr, *Physical Review B* **19**, 3808 (1979).
- [39] C. Brezinski, *Applied Numerical Mathematics* **20**, 299 (1996).
- [40] G. A. Baker Jr, *Physical Review* **124**, 768 (1961).
- [41] H. Mera, T. G. Pedersen, and B. K. Nikolić, *Phys. Rev. Lett.* **115**, 143001 (2015).
- [42] H. Mera, T. G. Pedersen, and B. K. Nikolić, *Phys. Rev. D* **97**, 105027 (2018).
- [43] É. Borel, Translated by Charles L. Critchfield and Anna Vaker (1975), Los Alamos Scientific Laboratory (1928).
- [44] W. Janke, *Resummation of Divergent Perturbation Series: Introduction to Theory & Guide to Practical Applications* (World Scientific, 1998).
- [45] The singularity structure of Σ can be rather involved [29] and is generally unknown.
- [46] R. Rossi, N. Prokof'ev, B. Svistunov, K. V. Houcke, and F. Werner, *EPL (Europhysics Letters)* **118**, 10004 (2017).
- [47] M. Troyer and U.-J. Wiese, *Phys. Rev. Lett.* **94**, 170201 (2005).
- [48] A. Moutenet, W. Wu, and M. Ferrero, *Physical Review B* **97**, 085117 (2018).
- [49] R. Rossi, arXiv:1802.04743 (2018).